

## Hard exclusive $\pi^0$ muoproduction at COMPASS

---

Markéta Pešková,<sup>a,\*</sup> Karolína Lavičková<sup>b</sup> and Nicole d'Hose<sup>c</sup>

<sup>a</sup>Charles university,

Ovocný trh 560/5, Prague, Czechia

<sup>b</sup>Czech Technical University in Prague,

Jugoslávských partyzánů 1580/3r, Prague, Czechia

<sup>c</sup>Irfu, CEA, Université Paris-Saclay,

91191 Gif-sur-Yvette, France

E-mail: [marketa.peskova@cern.ch](mailto:marketa.peskova@cern.ch), [karolina.lavickova@cern.ch](mailto:karolina.lavickova@cern.ch),

[nicole.dhose@cea.fr](mailto:nicole.dhose@cea.fr)

Hard Exclusive Meson Production and Deeply Virtual Compton Scattering (DVCS) are widely used reactions to study Generalized Parton Distributions (GPDs). Investigation of GPDs represents one of the main goals of the COMPASS-II program. Measurements of the exclusive processes were performed at COMPASS in 2016 and 2017 at the M2 beamline of the CERN SPS using the 160 GeV/c muon beam scattering off a 2.5 m long liquid hydrogen target surrounded by a barrel-shaped time-of-flight system to detect the recoiling target proton. The scattered muons and the produced real photons were detected by the COMPASS spectrometer, supplemented by an additional electromagnetic calorimeter for the detection of large-angle photons.

Exclusive  $\pi^0$  production is the main source of background for DVCS process, while it provides complementary information for parametrisation of GPDs. We will report on preliminary results on exclusive  $\pi^0$  production cross-section and its dependence on the squared four-momentum transfer  $|t|$  and on the azimuthal angle  $\phi$  between the scattering plane and the  $\pi^0$  production plane. The results will provide a further input to phenomenological models for constraining GPDs, in particular chiral-odd (“transversity”) GPDs.

41st International Conference on High Energy physics - ICHEP2022

6-13 July, 2022

Bologna, Italy

---

\*Speaker

## 1. Introduction

The General Parton Distributions (GPDs) represent one of the approaches beyond collinear approximation to describe the 3D partonic structure of a nucleon [1–5].

GPDs unify the momentum-space parton densities (PDFs) measured in inclusive deep-inelastic scattering with the spatial density (or Form Factors) measured in elastic scattering. They describe correlations between the momentum and spatial distributions of partons which is often mentioned as a 3D nucleon tomography, providing also access to fundamental static properties such as the quark orbital angular momentum..

There are eight GPDs for each parton flavour  $q$ , four parton helicity-conserving (chiral even) GPDs,  $H^q(x, \xi, t, Q^2)$ ,  $\tilde{H}^q(x, \xi, t, Q^2)$ ,  $E^q(x, \xi, t, Q^2)$ , and  $\tilde{E}^q(x, \xi, t, Q^2)$ , and four corresponding parton helicity-flip (chiral-odd or "transversity") GPDs:  $H_T^q(x, \xi, t, Q^2)$ ,  $\tilde{H}_T^q(x, \xi, t, Q^2)$ ,  $E_T^q(x, \xi, t, Q^2)$ , and  $\tilde{E}_T^q(x, \xi, t, Q^2)$ . Here,  $x$  denotes the average longitudinal momentum fraction of the struck quark with respect to the momentum of the nucleon target,  $\xi$  is half the change in the momentum fraction of the struck parton,  $t$  is the square of the four-momentum transferred to the target, and  $Q^2$  is the virtuality of the virtual photon  $\gamma^*$  exchanged between the lepton and the nucleon.

The GPDs are expected to be universal quantities, i.e. to be independent on the experimental process. Most commonly used processes for parametrisation of the GPDs are Deep Virtual Compton Scattering (DVCS) and Hard Exclusive Meson Production (HEMP). DVCS is particularly sensitive to GPDs  $H^q$ ,  $E^q$ ,  $\tilde{H}^q$ , and  $\tilde{E}^q$ . At a leading-twist, the vector and the pseudo-scalar meson productions by longitudinally polarised virtual photons are described by the GPDs  $H^q$  and  $E^q$ , and  $\tilde{H}^q$  and  $\tilde{E}^q$ , respectively. In particular, in the exclusive  $\pi^0$  production, the contribution from transversely polarised  $\gamma^*$  is expected to be suppressed by a factor of  $1/Q^2$  [6]. However, measurements of exclusive  $\pi^+$  production from HERMES experiment [7] and the exclusive  $\pi^0$  production from JLab CLAS and Hall A [8–10] have shown a significant contribution, and it is now widely accepted, that the transverse cross-section for exclusive  $\pi^0$  production is more important than expected. It can be explained as an effect of a chiral-odd GPD coupling to a twist-3 wave function, in the GPD formalism of ref. [11]. In the framework of the Goloskokov-Kroll phenomenological model, the pseudo-scalar meson production is described by the GPDs  $\tilde{H}^q$ ,  $\tilde{E}^q$ ,  $H_T^q$  and  $\tilde{E}_T^q = 2\tilde{H}_T^q + E_T^q$ . Different partonic contents of the produced mesons give different sensitivities to various GPDs and allow for flavour separation. The exclusive  $\pi^0$  production, in particular, is sensitive to the chiral-odd GPD  $\tilde{E}_T^q$ . The first results from the exclusive  $\pi^0$  production measurement at COMPASS from a short pilot run made in 2012 support this expectation [12].

The COMPASS GPD program comprises of a pilot run in 2012, and a main data-taking period in 2016 and 2017. The measurements were performed with polarised  $\mu^+$  and  $\mu^-$  beams scattering off an unpolarised liquid hydrogen target. The first preliminary results from the 2016 data on the exclusive  $\pi^0$  differential cross-section dependent on  $t$  and  $\phi$  are presented in this contribution, and compared to the updated Goloskokov-Kroll's model [17].

## 2. COMPASS spectrometer

COMPASS is a fixed-target experiment situated at the M2 beam-line of the CERN Super Proton Synchrotron (SPS). It supports both hadron and naturally longitudinally polarised muon beams with energies ranging between 50 and 280 GeV/c. For the GPD program the measurements were performed with 160 GeV/c  $\mu^+$  and  $\mu^-$  beams with a polarisation of -0.8 and +0.8, respectively [13].

COMPASS is a two-stage magnetic spectrometre comprising approximately 350 tracking planes, three electromagnetic and two hadronic calorimetres, two muon detectors and a ring-imaging Cherenkov detector for particle identification. The GPD program commenced with a four-weeks-long pilot run in 2012. The main data taking was performed in 2016 and 2017, collecting about nine times larger statistics than was collected in the pilot run. The COMPASS set-up has been complemented with a 2.5 m long liquid hydrogen target inserted in a proton recoil detector, CAMERA, and a new electromagnetic calorimeter for large azimuthal angles, ECAL0. The 4 m long proton recoil detector consists of 2 concentric barrels equipped with 24 scintillator slabs per barrel. The detection of recoiled proton is based on its time of flight between the two barrels. The ECAL0 calorimeter is placed directly downstream of the target and allows to expand the accessible kinematic domain for DVCS and HEMP measurement towards higher  $x_B$ , improving the efficiency of detecting the exclusive events and reducing the background. This set-up is capable of measuring the exclusive events within the kinematic domain from  $x_B \sim 0.01$  to 0.25, which is complementary to other experimental facilities.

## 3. Event selection

The event selection relies on the over-constrained kinematics for the measured exclusive process  $\mu p \rightarrow \mu' p_{recoil} \pi^0$ . The  $\pi^0$  mesons are identified by their dominant two-photon decay. Fig. 1 shows the invariant mass of the double-photon system for the  $\mu^+$  beam and the  $2.5\sigma$  cut applied on the  $\pi^0$  peak. The event candidates must contain two neutral clusters in the electromagnetic calorimeters, one reconstructed vertex within the liquid-hydrogen target with an incoming muon and an identified scattered muon, and a recoiled proton measured in CAMERA. For an event candidate, the kinematics of the recoil proton candidates are compared with the corresponding predictions that are obtained using spectrometer information only, utilizing the over-constraints of the measurement. Fig. 2 shows the kinematic variables used for this comparison and the applied cuts for the selection of events. The upper left panel of fig. 2 shows the difference between the measured and the predicted value of the recoiled proton transverse momentum  $\Delta p_T$ , for the  $\mu^+$  beam as an example, the upper right panel illustrates the difference of the azimuthal proton angle  $\Delta\varphi$ . Here,  $p_T$  and  $\varphi$  are measured in the laboratory system. The bottom left panel in fig. 2 represents the difference  $\Delta z$  between the longitudinal position of the hit in the inner CAMERA barrel  $z_A$  and the interpolated one between the interaction vertex position and the longitudinal position of the

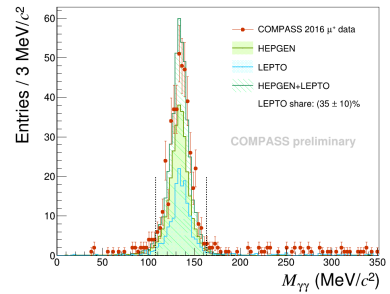


**Figure 1:** Invariant mass of the  $\gamma\gamma$  system, for the  $\mu^+$ , and the  $2.5\sigma$  cut on the  $\pi^0$  peak.

hit in the outer barrel  $z_B$ . Finally, the bottom right panel in fig. 2 shows the undetected mass:  $M_X^2 = (k + p - k' - q' - p')^2$ , where  $k$  and  $k'$  are the four-momenta of the initial and final muon, respectively,  $p$  and  $p'$  stand for the four-momenta of target and recoiled proton, respectively, and  $q'$  denotes the  $\pi^0$  four-momentum.

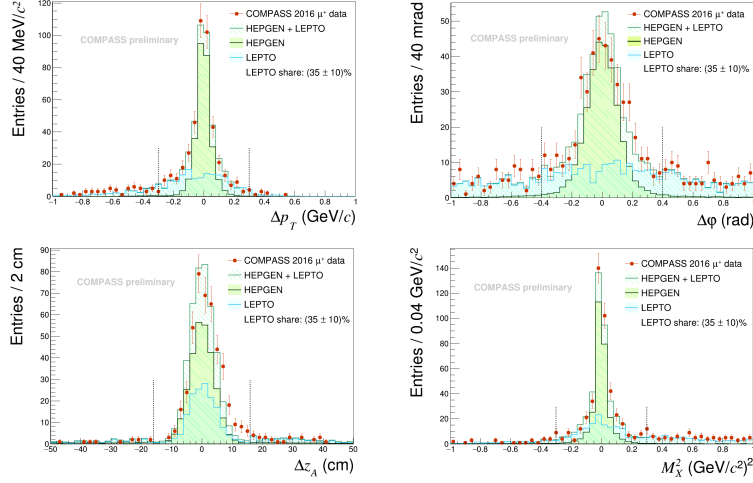


**Figure 2:** Distributions of the exclusivity variables for the  $\mu^+$ :  $\Delta p_T$  and  $\Delta\phi$  in the upper row, and  $\Delta z$  and the four-momentum balance in the lower row. The simulated non-exclusive  $\pi^0$  background is estimated using LEPTO (in blue), while the total  $\pi^0$  distribution is estimated using both LEPTO and HEPGEN (in dark green). Black dotted vertical lines indicate the applied cuts.

The main background to exclusive  $\pi^0$  production originates from non-exclusive deep-inelastic scattering (DIS) processes. The DIS background is estimated using the LEPTO simulation [15], while the signal events of exclusive  $\pi^0$  mesons are modelled by the HEPGEN++ simulation [16]. The signal (HEPGEN++) and the background (LEPTO) samples are first normalised to the data using the distribution of invariant  $\gamma\gamma$  mass around  $2.5\sigma$  of the  $\pi^0$  peak. The mixture of LEPTO and HEPGEN++ samples is subsequently fitted on the data using several kinematic variables to gain yields of each Monte Carlo sample. The sum of the respectively scaled HEPGEN and LEPTO fitted on the data is shown in fig. 2. The resulting fraction of non-exclusive (DIS) background is estimated to be  $(35 \pm 10)\%$ . The background fit method is estimated to be the main source of the systematic uncertainty and additional systematic studies are currently in progress.

## 4. Results

The differential cross-section of the exclusive  $\pi^0$  production as a function of  $|t|$ ,  $\phi$ ,  $\nu$ , and  $Q^2$  is gained by correcting collected events for the luminosity<sup>1</sup>, the spectrometer acceptance, and a background subtraction bin-by-bin. The differential  $\mu p$  cross-section is determined separately for

<sup>1</sup>Integral luminosity of the 2016 COMPASS data used for this analysis for  $\mu^+$  beam:  $L_{\mu^+} = 51.9 \times 10^{11} \text{ nb}^{-1}$ , and for  $\mu^-$ :  $L_{\mu^-} = 44.8 \times 10^{11} \text{ nb}^{-1}$

$\mu^+$  and  $\mu^-$  beams. The unpolarised  $\mu p$  cross-section is obtained by averaging over the two beam polarities. The reduced  $\gamma^* p$  cross-section is extracted from the unpolarised  $\mu p$  cross section by using the transverse virtual-photon flux  $\Gamma = \Gamma(E_\mu, Q^2, \nu)$  [12]:

$$\frac{d^4\sigma_{\mu p}}{dQ^2 d|t| d\nu d\phi} = \Gamma \frac{d^2\sigma_{\gamma^* p}}{d|t| d\phi} \quad (1)$$

Here,  $|t|$  denotes the square of the four-momentum transferred to the target in absolute value,  $\nu$  is the energy of the virtual photon  $\gamma^*$  and  $\phi$  is the angle between the muon scattering plane and the hadron production plane. The reduced unpolarised exclusive  $\pi^0$  production cross-section is formulated as follows:

$$\frac{d\sigma^{\gamma^* p}}{d|t| d\phi} = \frac{1}{2\pi} \left[ \frac{d\sigma_T}{d|t|} + \epsilon \frac{d\sigma_L}{d|t|} \epsilon \cos(2\phi) \frac{d\sigma_{TT}}{d|t|} + \sqrt{2\epsilon(1+\epsilon)} \cos(\phi) \frac{d\sigma_{LT}}{d|t|} \right], \quad (2)$$

where  $\sigma_T$ ,  $\sigma_L$ ,  $\sigma_{TT}$ , and  $\sigma_{LT}$  are structure functions,  $\epsilon$  denotes the virtual photon polarisation. The subscript T(L) marks the contribution from transversely (longitudinally) polarised  $\gamma^*$ , the subscripts TT and LT signify the interference terms between transversely-transversely and longitudinally-transversely polarised photons. The structure functions from the eq. (2) are connected to convolutions of GPDs with functions describing the interaction of the virtual photon with the active quarks, for details see e.g. [11, 12]. The results of the  $\phi$ -dependent exclusive  $\pi^0$  cross-section averaged over the measured  $|t|$ -range, and the  $|t|$ -dependence after the integration over  $\phi$  are presented in fig. 3.

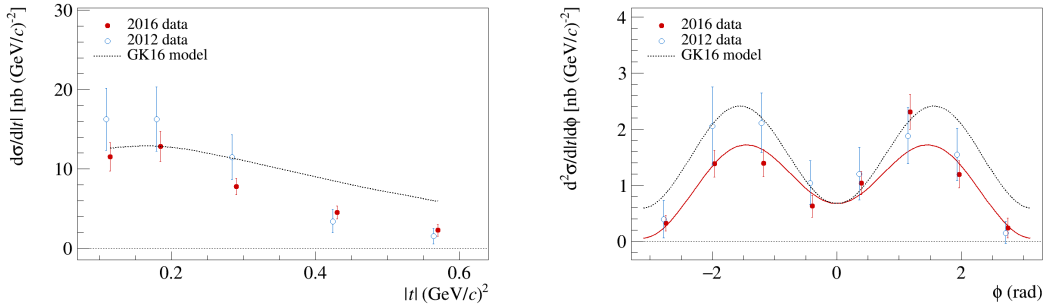


**Figure 3:** **Left:** The exclusive  $\pi^0$  cross section as a function of  $|t|$ . **Right:** The exclusive  $\pi^0$  cross section as a function of  $\phi$ . Preliminary results using the 2016 data are represented by the red dots, published results from the 2012 data [12] are shown in blue empty circles and the black dash-dotted line denotes the Goloskokov-Kroll (GK) parametrisation [17]. Only the statistical errors are shown on the 2016 data.

The analysis was performed on the background-corrected data sample collected in the 2016 run with average kinematics:  $\langle Q^2 \rangle = 2.07$  (GeV/c) $^2$ ,  $\langle \nu \rangle = 12.6$  GeV,  $\langle |t| \rangle = 0.281$  (GeV/c) $^2$ ,  $\langle W \rangle = 4.74$  (GeV/c), and  $\langle x_B \rangle = 0.096$ . Our results were compared to the current version of the Goloskokov-Kroll model, represented by the dashed-dotted curve [17], which was updated from the original version from 2011 [11] implementing the 2012 COMPASS results [12]. The new input of the 2016 results can serve to further constrain the Goloskokov-Kroll model, as well as other phenomenological models.

## 5. Outlook

The results presented in this contribution represented about 2.3 times higher statistics than in the published 2012 results. Over the full two-year data-taking COMPASS collected about 9 times more statistics than in the 2012 pilot run. The analysis of the COMPASS data collected in 2017 is currently ongoing and the plan is to include the whole set of statistics and proceed for publication in a near future, providing further constraints for the Goloskokov-Kroll model.

**Acknowledgements** This work is supported by Charles University grant GAUK 60121, and the grant SVV No. 260576.

## References

- [1] D. Müller, D. Robaschik, B. Geyer, F. M. Dittes, and J. Hořejší, *Fortsch. Phys.* **42** 101 (1994)
- [2] X. D. Ji, *Phys. Rev. Lett.* **78** 610 (1997)
- [3] X. D. Ji, *Phys. Rev. D* **55** 7114 (1997)
- [4] A. V. Radyushkin, *Phys. Lett. B* **385** 333 (1996)
- [5] A. V. Radyushkin, *Phys. Lett. D* **56** 5524 (1997)
- [6] J. C. Collins, L. Frankfurt, and M. Strikman, *Phys. Lett. D* **56** 2982 (1997)
- [7] A. Airapetian, *et al.* (HERMES Collaboration), *Phys. Lett. B* **659** 486 (2008)
- [8] I. Bedlinskiy, *et al.* (CLAS collaboration), *Phys. Lett. C* **90** 025205 (2014)
- [9] M. Defurne, *et al.* (Hall A collaboration), *Phys. Rev. Lett.* **117** 262001 (2016)
- [10] M. Dlamini, *et al.* (Hall A collaboration), *Phys. Rev. Lett.* **127** 152301 (2021)
- [11] S. Goloskokov, and P. Kroll, *Eur. Phys. J. A* **47** 112 (2011)
- [12] M. G. Alexeev, *et al.* (COMPASS collaboration), *Phys. Lett. B* **805** 135454 (2020)
- [13] F. Gautheron, *et al.* (COMPASS collaboration) CERN-SPSC-2010-014, SPSC-P-340 (2010)
- [14] M. Gorzellik, Cross-section measurement of exclusive  $\pi^0$  muoproduction and firmware design for an FPGA-based detector readout (University of Freiburg) doi:106094/UNIFR/15945 (2018)
- [15] G. Ingelman, A. Edin, J. Rathsman, *Computer Physics Communications* **101**, Issues 1–2 (1997)
- [16] A. Sandacz, and P. Sznajder, arXiv:1207.0333 [hep-ph] (2012)
- [17] S. Goloskokov, and P. Kroll, private communications (2016)